Chapter 7

Arene–Arene Double T-Contacts: Lateral Synthons in the Engineering of Highly Anisotropic Organic Molecular Crystals

Michael Lewis, Zhengyu Wu, and Rainer Glaser*

Department of Chemistry, University of Missouri at Columbia, Columbia, MO 65211

An arene-arene double T-contact describes a pair of intermolecular arene-arene T-contacts between two molecules that each contain two spacer-connected arene rings. We have been employing such double T-contacts as lateral synthons in the crystal engineering of highly anisotropic organic crystals. In particular, this type of intermolecular interaction has been employed as a stabilizing factor to overcome the intrinsic preference for the anti-parallel alignment of dipolar molecules. Here, we review pertinent properties of benzene and of the benzene-benzene interaction and present and discuss arene-arene double T-contacts in crystals of a representative number of symmetrical and unsymmetrical acetophenone azines, $X–C_6H_4–CMe=N–N=CMe–C_6H_4–Y$, including the structures of two near-perfectly dipole parallel-aligned crystals.

Introduction

For materials to exhibit NLO activity (*1*) two physical properties are essential. First, a crystal must be asymmetric. For organic crystals, this prerequisite is relatively easy to meet because 20% of all organic molecules crystallize in chiral space groups (*2*). The second and much more challenging criterion for a crystal to be NLO active is the presence of a macroscopic dipole moment. This is not trivial, because most polar

[1]Corresponding author.

Glaser and Kaszynski; Anisotropic Organic Materials
ACS Symposium Series; American Chemical Society: Washington, DC, 2001.

molecules tend to pack such that their dipole moments cancel each other (Scheme 1a), thus giving a crystal dipole moment of zero. Most crystals that exhibit a non-zero dipole moment do so because of an incomplete cancellation of the molecular dipole moments (Scheme 1b). In those cases, the crystal dipole moment is considerably less than the sum of the molecular dipole moments and such cases are far from ideal. The most desirable result is perfect dipole alignment (Scheme 1c) so that the dipole moment of the crystal is equal of at least approximately equal to the sum of the individual molecules.

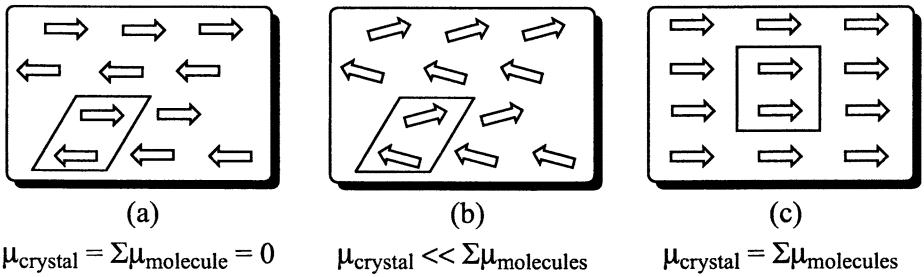

Scheme 1. (a) Complete cancellation, (b) incomplete or partial cancellation and (c) complete reinforcement of molecular dipole moments.

While the interest in polar organic materials has been tightly linked to applications in nonlinear optics, highly polar crystalline materials are of interest in and of themselves. Molecular orientation and parallel dipole alignment is important for many optical and electrical applications. A polar, anisotropic environment is key for nonlinear optical responses in crystals (*vide supra*) and in liquid crystals (*3*, *4*, *5*). Similarly, the NLO activity of dyes in polymer films depends on the parallel alignment of molecular dipole moments (*6*). Other optical phenomena that depend on molecular anisotropy include thermal conductivity (*7*), ferroelectric responses (*8*) and ferroelastic responses (*9*). From a fundamental point of view, our materials will allow for systematic studies of the effects of a highly polar environment on molecular properties. The polar alignment of the molecules will cause large electric fields within the crystals and the properties of the free molecule and of the molecule in the crystal can be expected to be quite different. It is possible to measure internal electric fields with atomic resolution (*10*, *11*) and our work might enable systematic studies of internal electric fields in polar crystals.

We have designed donor-acceptor-substituted π-conjugated molecules (Scheme 2) aimed at overcoming the parallel dipole alignment challenge by incorportating structural motifs that enhance the likelihood of obtaining the scenario illustrated in Scheme 1c. The first key issue of our design concept is the minimization of the ground state dipole moment. Relatively small ground state dipole moments are required to minimize the intrinsic advantage of the dipole antiparallel-aligned arangement over the dipole parallel-aligned arrangement. This design feature is

accomplished by placing an azine bridge in the center of the molecule. The azine bridge can be viewed as two polar acceptor imine groups with opposite orientations, and thus acts as a conjugation stopper (*12*) (Scheme 2). The imine-acceptor conjugation in one half of the molecule results only in a very small contribution to the overall dipole moment for that segment. The overall dipole moment is largely due to the donor-imine conjugation. Our *ab initio* studies have shown that the azine bridge is effective in preventing through-conjugation when placed between donor- and acceptor-substituted π-systems (*12*) and extensive NMR studies fully support this view (*13*). The second important design concept is the use of aromatic systems as alignment units (Scheme 2). Intermolecular arene-arene interactions (*vide infra*) are employed to compensate for electrostatic repulsions of parallel dipole alignment.

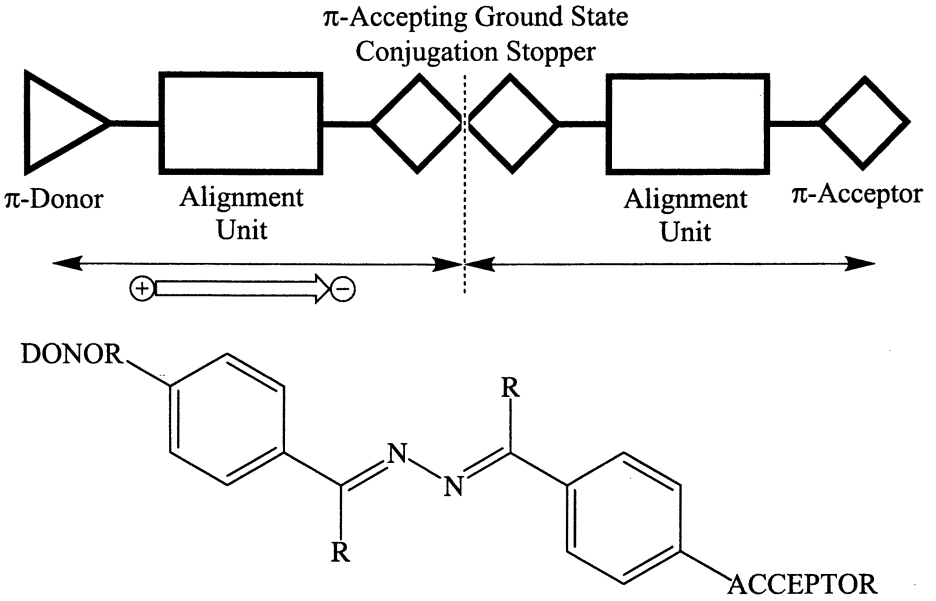

Scheme 2. Dipole design concept. The azine bridge acts as a π-accepting conjugation stopper and the phenyl rings function as lateral synthons whose intermolecular interactions help to overcome the intrinsically preferred antiparallel dipole alignment of molecular dipoles.

In this context we have been investigating the stereochemistry (*14*, *15*, *16*), electronics (*12*, *14*, *16*) and crystal packing (*14*, *16*, *17*, *18*, *19*, *20*, *21*) of symmetric and unsymmetric acetophenone azines with aims at overcoming the dipole alignment challenge. The azines that we have studied have the general structure shown in Scheme 2. All of the crystal structures we have obtained thus far have intermolecular double arene-arene interactions as the dominant packing motif thus underscoring the importance of arene-arene interactions in controlling the packing. A double arene-

arene interaction occurs when two arene rings of one molecule interact with the two arene-arene rings of an adjacent molecule. In this chapter, we will briefly review the literature on pertinent properties of benzene and of the benzene-benzene interaction and present and discuss arene-arene double T-contacts in crystals of a representative number of symmetrical (X = Y) and unsymmetrical (X ≠ Y) acetophenone azines, X–C_6H_4–CMe=N–N=CMe–C_6H_4–Y, including the structures of two near-perfectly dipole parallel-aligned crystals.

Benzene Structure and Quadrupole Moment

Benzene has only one unique diagonal traceless quadrupole moment tensor component, Θ_{zz} (*z*-axis is symmetry axis), which can be measured via electric field gradient induced birefringence (*22*) and diode laser spectroscopy (*23*). The most recent measurement is that of Sumpf (*23*) which gave $\Theta_{zz} = -1.0 \bullet 10^{-25}$ esu. This value is close to the frequently cited value of $\Theta_{zz} = -6.47 \pm 0.37$ a.u. reported in 1981 by Battaglia and Buckingham from birefringence data (*22*). Because the birefringence method is the most popular way for the determination of quadrupole moments, we use that experimental value for comparison to our *ab initio* calculations.

The first structure determination of benzene was that of Cox (*24*) in 1932; X-ray diffraction of a single crystal at -22°C showed a D_{6h} structure with a CC bond length of about 1.42 Å. The most precise structural work is the electron diffraction study of Strand (*25*) which yielded equilibrium distances r_e(CC) = 1.3929 Å and r_e(C–H) = 1.0857 Å and we used this geometry for our benzene quadrupole moment (single point) calculations. Results of our calculations of the quadrupole moment of benzene are given in Table 1 (*26*). All unabridged quadrupole moment tensor components are negative. The negative charge (electrons) is distributed further from the center of mass than the positive charge (nuclei) and the quadrupolarity of benzene molecule can thus be characterized as {- + -} in every direction. Q_{zz} is about 25% larger in magnitude than Q_{xx} and Q_{yy}. Compared with the experimental value –6.47 ± 0.37 au (*22*), our data fall into a ±10% error range. RHF/cc-pVDZ and RHF/cc-pVDZ++ give the closest values. The choice of a good basis set is the most critical issue.

Table I. Quadrupole Moment Tensor Components and Quadrupole Moment

Method/Basis Set	$Q_{xx}=Q_{yy}$[a]	Q_{zz}[a]	$<Q_{ii}>$[a]	Θ[a]	Θ[b]	%Error
RHF/6-311G(d,p)	-31.670	-40.631	-34.657	-8.962	-6.663	3.137
RHF/6-311++G(d,p)	-31.936	-41.319	-35.063	-9.383	-6.976	7.991
RHF/6-311G(2d,p)	-31.532	-40.409	-34.491	-8.877	-6.600	2.166
RHF/6-311++G(2d,p)	-31.835	-41.251	-34.974	-9.415	-7.000	8.359
RHF/cc-pVDZ	-31.775	-40.381	-34.644	-8.606	-6.398	-0.956
RHF/cc-pVDZ++	-31.671	-40.504	-34.615	-8.833	-6.567	1.654
MP2/6-311G(d,p)[c]	-32.240	-39.972	-34.817	-7.732	-5.748	-11.014
MP2/6-311++G(d,p)[c]	-32.540	-40.779	-35.286	-8.239	-6.126	-5.174

[a]Units in DÅ. [b]Units in a.u. [c]MP2 active space included all electrons.

Benzene-Benzene Interactions

The structure of benzene dimer has been studied theoretically (*27*) and experimentally (*28*) in the gas-phase, solution-phase and the solid state and all results suggest that the edge-to-face structure, or T-contact (**A** and **B** in Scheme 3), is more stable than the parallel-displaced face-to-face structure (**C**). The T-shaped structure can form numerous geometries, two of which are shown as **A** and **B** in Scheme 3 with the most stable structure being **A**.

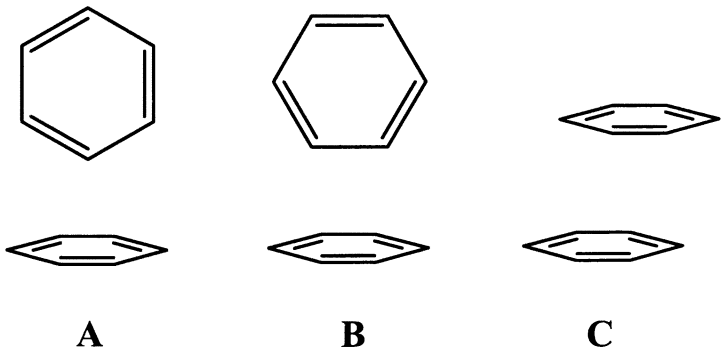

Scheme 3. (a) Edge-to-face contact or T-contact with one C-H pointing toward the benzene π-cloud. (b) T-contact with two C-H bonds pointing to the π-cloud. (c) Off-set face-to-face contact.

Initial *ab initio* gas-phase calculations at the MP2/MIDI-1+s,p(c) level of theory (*29*) suggested that there were four energy minima on the benzene dimer potential energy surface (PES). Three of the four structures were T-shaped with the most stable one illustrated by **A** and the fourth structure was the parallel-displaced face-to-face structure **C**. The most stable T-structure had an intermolecular distance of 5.0 Å between the molecular centers and was more stable than the parallel-displaced face-to-face structure with an intermolecular distance of 4.3 Å by approximately 0.4 kcal/mol (*29*). Later calculations using the better 6-31+G* (*30*) and DZ+2P (*31*) basis sets in conjunction with the MP2 method found that the parallel-displaced face-to-face structure was more stable by 0.9 and 0.2 kcal/mol, respectively. The intermolecular distance for the T-shaped structure was the same as the MP2/MIDI-1+s,p(c) calculations, 5.0 Å between the molecular centers, however the parallel-displaced face-to-face structure had much closer intermolecular distance of 3.85 Å. The fact that the T-shaped and parallel-displaced structures of benzene are nearly isoenergetic was reaffirmed using higher levels of theory, MP4 and CCSD(T), and better basis sets, AUG-cc-pVDZ (*32*). The CCSD(T)/AUG-cc-pVDZ calculations have intermolecular distances of 5.1 and 4.0 Å between the molecular centers for the T-shaped and parallel-displace face-to-face structures, respectively. The most recent

CCSD(T) dynamics calculations on the benzene dimer (*33*) suggest that there exists only one minimum on the PES and it is the T-structure. This study located four other stationary points, however they were either first or second order saddle points. The parallel-displaced face-to-face structure **C** was found to be a transition state for the automerization of the T-structure. The intermolecular distance between the molecular centers for the T-shaped structure in this study was 5.21 Å. The T-structure was also calculated to be more stable than the face-to-face structure in aqueous solution (*34*) and liquid benzene (*35*) via molecular dynamics and Monte Carlo simulations, respectively. The predominant structure for the calculations of liquid benzene is T-shaped with an intermolecular distance of 5.5 Å between the molecular centers. Finally, molecular mechanics calculations aimed at simulating the benzene crystal also predict the T-shaped structure to be most stable (*36*) with intermolecular distances of approximately 5.0 Å.

The large body of experimental work on benzene dimer also points to the T-shaped structure being more stable than the face-to-face aggregate. Early work employed electric deflection measurements (*37*, *38*) to show that benzene dimer possesses an electric dipole moment, thus ruling out face-to-face structure and suggesting a T-shaped one. A T-shaped structure was also hypothesized by mass-selective two-photon ionization experiments (*39*) and molecular jet optical absorption spectra (*40*). The latter study went so far as to suggest a C_{2v} symmetry for the T-shaped benzene dimer, however, subsequent time-of-flight multiphoton mass spectra (*41*) revealed that the two benzene rings were not perpendicular but rather they deviated from orthogonality by 10°-20°. A binding energy of 1.6 ± 0.23 kcal/mol was determined for this arrangement using a reflection time-of-flight mass spectrometer after two-photon ionization (*42*). More recent mass-selective Raman spectroscopic studies (*43*, *44*) and mass-selective hole-burning experiments (*45*) also point to a floppy T-shaped structure, however one such mass-selective Raman study (*46*) reports the presence of both an edge-to-edge and a T-shaped structure with intermolecular distances of 3.7-4.2 and 5.0 Å, respectively. A more precise intermolecular distance of 4.96 Å was reported for the T-shaped dimer using Balle/Flygare Fourier transform microwave spectroscopy (*47*). NMR spectroscopic measurements of neat benzene (*48*) show the presence of both the T-shaped and face-to-face structures with the T-shaped structure being favored by approximately 0.7 kcal/mol. The experimental data on solid state benzene unambiguously reflects the preference for the T-shaped structure. Benzene crystallizes into two unique lattices; benzene I is orthorhombic with the space group *Pbca* and benzene II is monoclinic with space group $P2_1/c$. The crystal structure of benzene I was determined by X-ray crystallography at –3°C (*49*) and by neutron diffraction at –55 and –135°C (*50*) and the benzene molecules pack at almost perfect right angles, 90°22', with intermolecular closest contacts of approximately 2.75 Å (*49*). Crystals of benzene II were grown and examined at 21°C and 25 kilobars (*51*). The closest intermolecular contacts in benzene II are similar to those in benzene I however the molecules are no longer orthogonal and they pack such that the planes of the two rings are at 120° angle with respect to each other (*51*).

Intermolecular Arene-Arene Double T-Contacts

The prevalent geometric motif of intermolecular interaction in our crystals is the arene-arene double T-contact. A double T-contact occurs when two phenyl rings of one molecule interact with the two phenyl rings of an adjacent molecule to produce two T-contacts. Arene-arene double T-contacts can achieve numerous arrangements and three of them are shown in Scheme 4. Pattern α can only occur when the space group connecting the phenyl rings is not twisted and the two phenyl rings within each molecule lie in the same plane. Patterns β and γ are two of the numerous motifs that result from a twisted spacer group with orthogonal or nearly orthogonal phenyl rings.

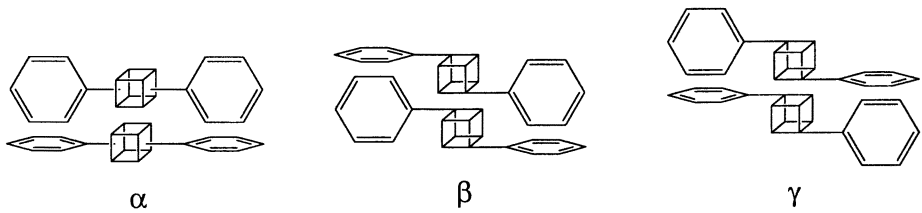

Scheme 4. Three possible double T-contacts between molecules with two spacer-connected arene units.

The azine bridge we employ in our dipolar molecules is the twisted spacer. This may seem contrary to simple notions of conjugation and valence bond theory, however it is in line with our theoretical view of the azine bridge as a conjugation stopper. The twisted nature of the azine bridge is not just a result of packing effects in the crystal, but rather it is an intrinsic property that is also witnessed for the free molecules in the gas phase and in solution. Quantum mechanical *ab initio* calculations show that the optimal structure of our azines in the gas phase is a twisted structure (*12*) and extensive NMR studies supporting this view (*13*). The twisted geometry of the azine bridge in our molecules precludes the formation of double T-contacts of the α-type (Scheme 4). Instead, all of the double T-contacts that we observe in our crystals have the general motif described by types β and γ. It is important to recognize that β and γ are structural isomers or association isomers because the β aggregate can be converted into the γ aggregate by moving the top molecule to the bottom.

Double T-Contacts Between Acetophenone Azines

The crystal structures of all of our azines are highly anisotropic and they only exist in parallel or antiparallel dipole aligned arrangements. One of the driving forces behind this high degree of orientational order is the double T-contact; double T-contacts are the dominant structural motif in every structure. The β- and γ-type double T-contacts

for selected symmetric acetophenone azines are shown in Figures 1 and 2 and the double T-contacts for selected unsymmetric azines are given in Figures 3 and 4. In all cases, each azine engages in *both* β- and γ-type double T-contacts.

Symmetric azines carry two identical substitutents and the three azines shown in Figures 1 and 2 are the parent compound (**H-H**) and the Cl- and I-substituted molecules (**Cl-Cl** and **I-I**). The key factor governing the formation of the double T-contact is the twisted azine spacer group. The three azines all assume a *gauche* conformation with –C=N–N=C– dihedral values, τ, of 138.7°, 134.7° and 141.8° for **H-H**, **Cl-Cl** and **I-I**, respectively. The dihedral angles relating the twist of the two phenyl rings with respect to the C_{para}-C_{imine} bond planes, ϕ_1 and ϕ_2, are 0.3° and 19.7° for **H-H**, 29.3° and 30.5° for **Cl-Cl**, and 8.0° and 8.0° for **I-I**. In all of our azines the N–N and the two C_{para}-C_{imine} bonds are almost parallel. Therefore, the sum of τ' (where $\tau' = 180 - \tau$), ϕ_1 and ϕ_2 provides an excellent approximation for the angle ω between the best planes of the benzene rings. The ω values for **H-H**, **Cl-Cl** and **I-I** are 61.3°, 105.1° and 54.2° and these angles can be visualized by looking down the N–N bonds as shown on the right side of Figures 1 and 2.

The two monomers in each β- and γ-type double T-contact are stereoisomers and they can be described by the *P*/*M* nomenclature for helicity (*52*). In this nomenclature the molecule has *P*-helicity if the shortest rotation around the N–N bond that results in an eclipsing of the phenyl rings is a clockwise rotation. Conversely, if the shortest rotation to effect eclipsing of the phenyl rings is counter-clockwise, then the molecule has *M*-helicity. For the dimers in Figures 1 and 2 the *P*-stereoisomer is always on top and the *M*-stereoisomer is on the bottom. The views on the right of Figures 1 and 2, looking down the N–N bonds, are illustrate the *P*- and *M*-helicities in the most compelling fashion.

The β- and γ-type double T-contacts formed in the crystal structure of **Cl-Cl** are very different than those formed in the crystal structures of **H-H** and **I-I**. The β-type double T-contacts (Figure 1) in **H-H** and **I-I** are arranged so that the CC aromatic bond that is *anti* to the N–N bond in the *P*-stereoisomer is in contact with the C-C aromatic bond that is *anti* to the N–N bond in the *M*-stereoisomer. In contrast, the β-type double T-contacts in **Cl-Cl** are arranged so that the aromatic CC bond that is *syn* to the N–N bond in the *P*-stereoisomer is in contact with the aromatic CC bond that is *anti* to the N–N bond in the *M*-stereoisomer. Likewise, a similar difference exists between the γ-type double T-contacts in the **H-H** and **I-I** crystal structures and those in the **Cl-Cl** crystal structure. The γ-type double T-contacts in **H-H** and **I-I** (Figure 2) have the CC aromatic bond that is *syn* to the N–N bond in the *P*-stereoisomer in contact with the CC aromatic bond that is *syn* to the N–N bond in the *M*-stereoisomer. The γ-type double T-contacts in the **Cl-Cl** crystal structure, however, are between the CC aromatic bond that is *anti* to the N–N bond in the *P*-stereoisomer and the CC aromatic bond that is *anti* to the N–N bond in the *M*-stereoisomer. Note that in all three structures each azine partakes in at least one β-type and one γ-type double T-contact. Therefore, both the *syn* and *anti* aromatic CC bonds of each azine partake in a double T-contact. The double T-contacts in **H-H**, **Cl-Cl** and **I-I** deviated from orthogonality by 30°, 15° and 35°, respectively, and this is similar to what is observed

in experimental work on benzene dimers in the gas phase (*41*, *43*, *44*, *45*). Gas phase experiments predicted a deviation of 10° to 20° from orthogonality and the crystal structure of benzene II has T-contacts that deviate about 30° from perpendicularity.

The double T-contacts in the other symmetric acetophenone azines that we have studied have the same general motif as those illustrated in Figures 1 and 2. The double T-contacts in the crystal structure of 4-bromoacetophenone azine have the same general structure as those in the symmetric **Cl-Cl** structure. The crystal structures of the symmetric 4-fluoro- and 4-methoxy-substituted acetophenone azines have double T-contacts that resemble those in **H-H** and **I-I**.

The crystal structures of the unsymmetrical acetophenone azines that we have studied all exhibit similar double T-contacts to those in **H-H** and **I-I**. Three examples

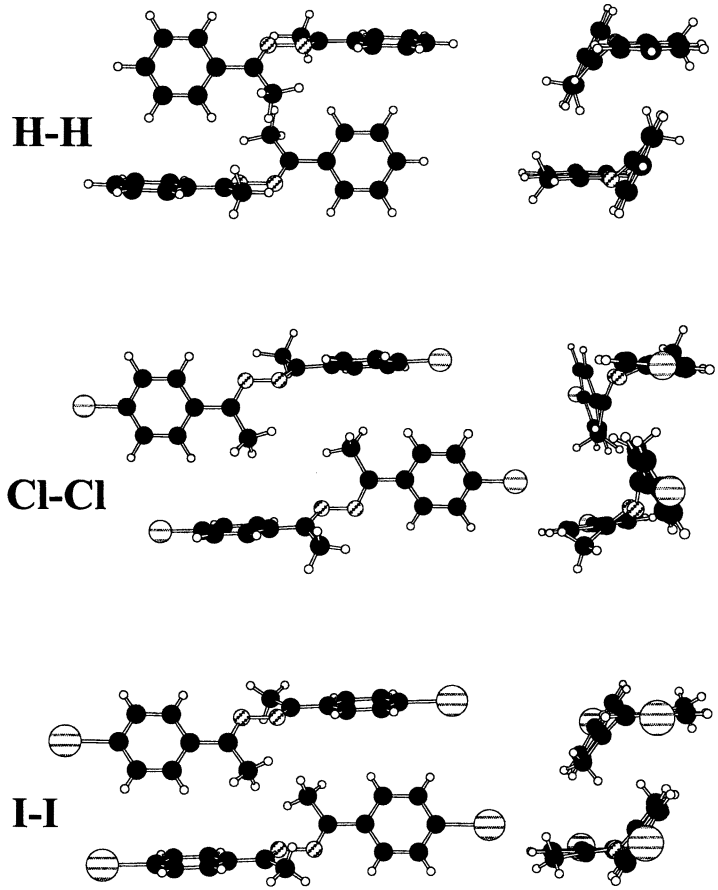

Figure 1. Illustration of β-type double T-contacts in the X-ray crystal structures of selected symmetric acetophenone azines. P-stereoisomers are on top and the M-stereoisomers are on the bottom.

of unsymmetrical donor-acceptor-substituted acetophenone azine double T-contacts are shown in Figure 3 and 4. Two of the examples have a methoxy group as the donor substituent and bromine and chlorine as the acceptors, **MeO-Br** and **MeO-Cl**, and one has an amino group as the donor and a nitro group as the acceptor, **NH_2-NO_2**. The β-type double T-contacts formed by these three crystal structures are shown in Figure 3 and the γ-type double T-contacts are illustrated in Figure 4.

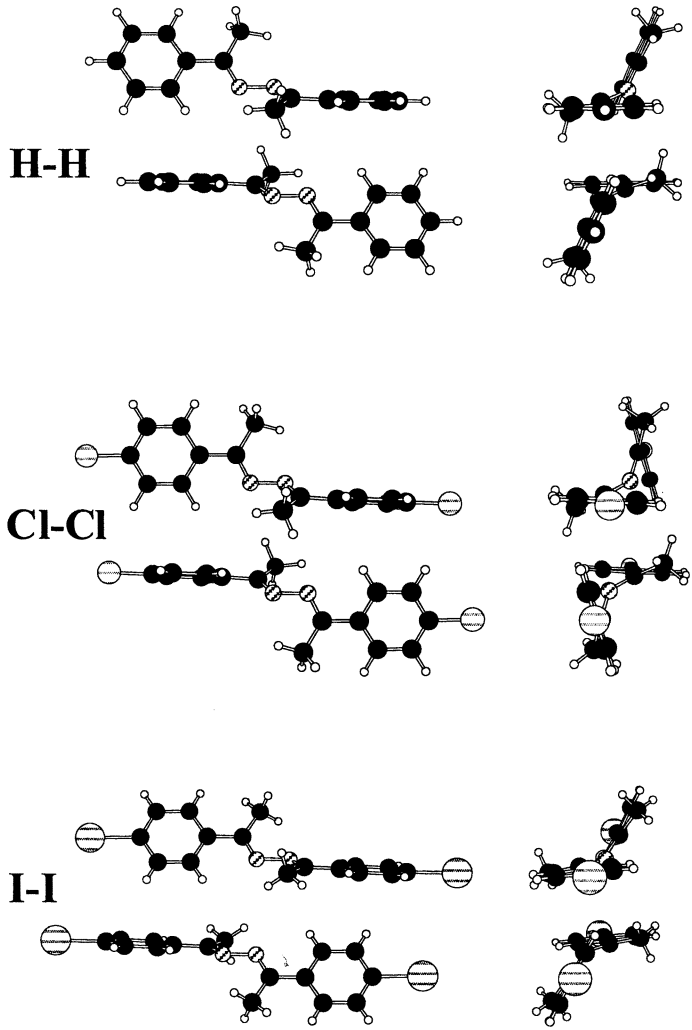

Figure 2. Illustration of γ-type double T-contacts in the X-ray crystal structures of selected symmetric acetophenone azines. P-stereoisomers are on top and the M-stereoisomers are on the bottom.

In the same fashion as the symmetric azines, the double T-contacts of the unsymmetrical azines are a result of the *gauche* conformations of the two phenyl groups within each monomer. As was the case for the symmetric azines, the –C=N–N=C– dihedral values, τ, are not always the same for the *P*- and *M*-stereoisomers. For **MeO-Br** and **MeO-Cl** the *P*- and *M*-stereoisomers do not have the exact same structure. The τ-values for **MeO-Br** are 135.8° for the *P*-isomer and 137.4° for the *M*-isomer and for **MeO-Cl** the values are 134.7° and 136.5°. The *P*- and *M*-stereoisomers in $\mathbf{NH_2}$-$\mathbf{NO_2}$ are isostructural and the τ value is 135.5°. Defining the dihedral angles that relate the twist of the two phenyl rings with respect

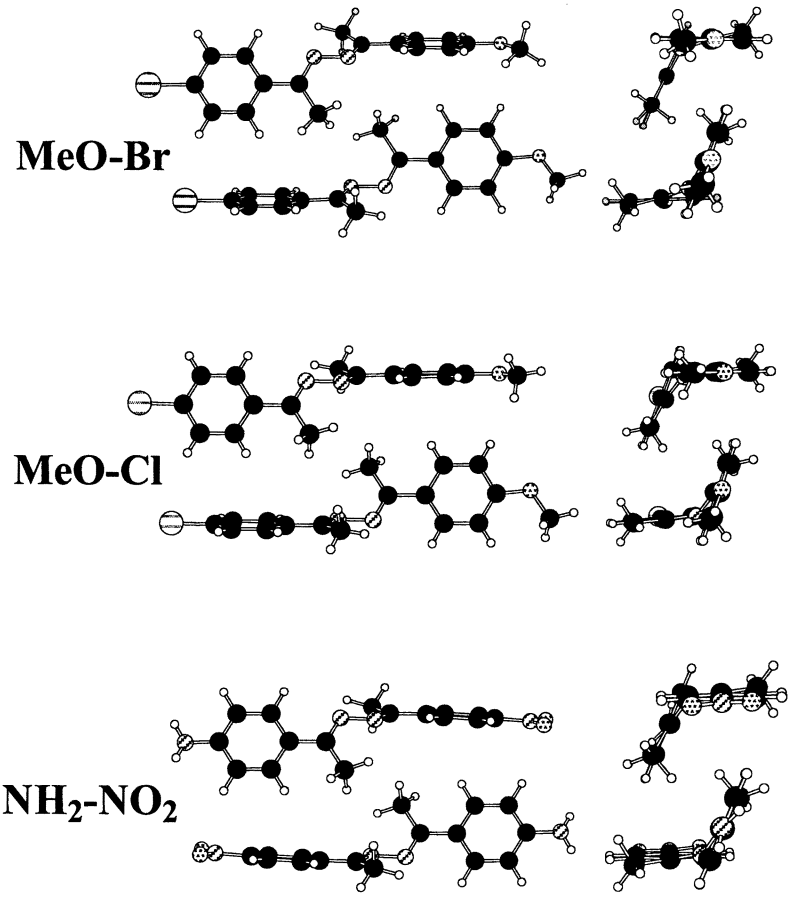

Figure 3. Illustration of β-type double T-contacts in the X-ray crystal structures of selected unsymmetric acetophenone azines. P-stereoisomers are on top and the M-stereoisomers are on the bottom.

to the C_{para}–imine bond planes, ϕ_1 and ϕ_2, becomes less arbitrary when the azine is not symmetric and we assign ϕ_1 to the phenyl ring with the donor substituent and ϕ_2 to the acceptor-substituted ring. For **MeO-Br** the ϕ_1 values are 17.4° for the *P*-isomer and 8.7° for the *M*-isomer and the ϕ_2 values are 2.6° (*P*-isomer) and 13.6° (*M*-isomer). The values for **MeO-Cl** are 15.4° (ϕ_1, *P*-isomer), 7.9° (ϕ_1, *M*-isomer), 3.3° (ϕ_2, *P*-isomer) and 14.3° (ϕ_2, *M*-isomer). The ϕ_1 and ϕ_2 values for **NH_2-NO_2** are 10.7° and 8.1°, respectively. Thus, the angle ω between the best planes through the benzene

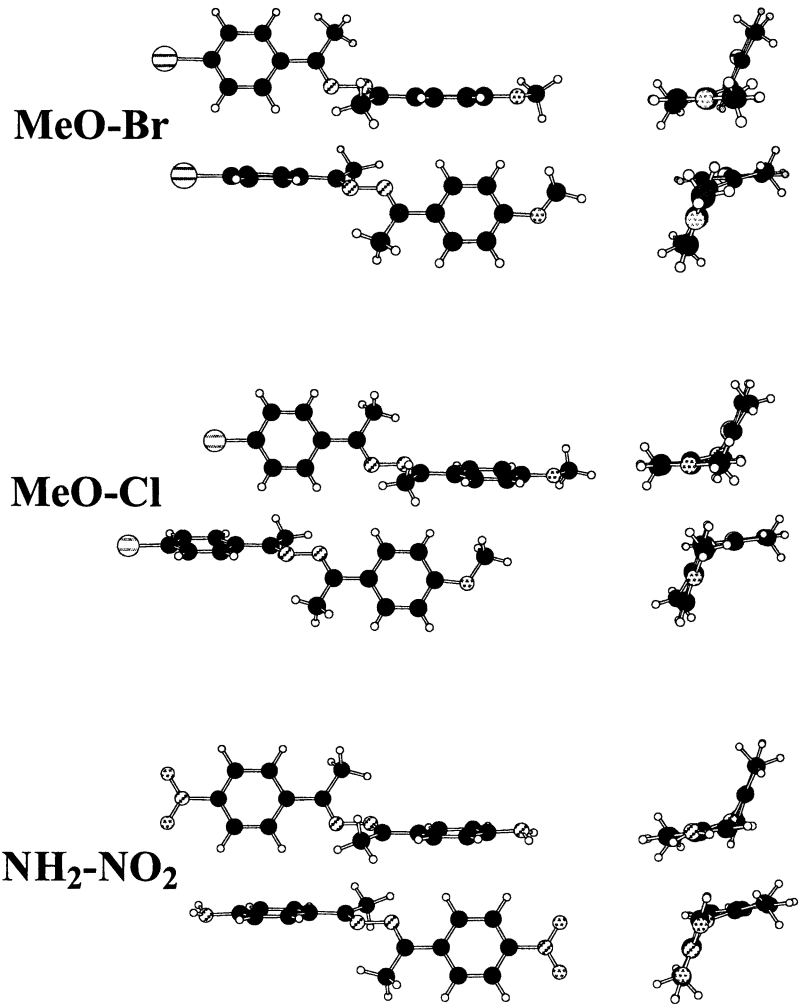

Figure 4. Illustration of the γ-type double T-contacts in the X-ray crystal structures of selected unsymmetric acetophenone azines. P-stereoisomers are on top and the M-stereoisomers are on the bottom.

rings for **MeO-Br** is 64.2° for the *P*-isomer and 64.9° for the *M*-isomer. For **MeO-Cl** the ω values are 64.0° and 65.7° for the *P*- and *M*-stereoisomers, respectively. The ω value for **NH_2-NO_2** is 63.3°. These angles are best visualized via the Newman-type views down the N–N bonds shown on the right side of Figures 3 and 4.

The β- and γ-type double T-contacts formed in the crystal structures of **MeO-Br**, **MeO-Cl** and **NH_2-NO_2** all have the same motif as those formed in the crystal structures of **H-H** and **I-I**. The β-type double T-contacts of **MeO-Br**, **MeO-Cl** and **NH_2-NO_2** (Figure 3) are arranged so that the CC aromatic bond that is *anti* to the N–N bond in the *P*-isomer is in contact with the CC aromatic bond that is *anti* to the N–N bond in the *M*-isomer. The γ-type double T-contacts in **MeO-Br**, **MeO-Cl** and **NH_2-NO_2** (Figure 4) have the CC aromatic bond that is *syn* to the N–N bond in the *P*-isomer in contact with the CC aromatic bond that is *syn* to the N–N bond in the *M*-isomer. As was the case for the symmetrical azines, the *syn* and *anti* aromatic CC bonds of each unsymmetrical azine monomer partake in at least one β-type and one γ-type double T-contact. The double T-contacts in the three unsymmetrical acetophenone azine crystal structures shown in Figures 3 and 4 all deviate from orthogonality by 20° to 25° and this further supports the experimental and theoretical preference for non-perpendicular arene-arene T-structures. The crystal structures of other donor-acceptor-substituted mixed acetophenone azines studied in our group also contain monomers with *gauche* conformations and the dimers form similar motifs as in **MeO-Br**, **MeO-Cl** and **NH_2-NO_2**.

Summary

The quadrupole moment of benzene is significant and we employ this property of aromatic systems in the design of parallel dipole aligned materials. The intrinsic conformational preferences and flexibility of azines allow for optimal intermolecular double T-contacts. The dipole moment in all of our mixed azines is along the N–N bond and thus, Figures 3 and 4 illustrate the near perfect parallel dipole alignment in the crystal structures of **MeO-Br** and **MeO-Cl**. The molecular dipole moments of the **MeO-Hal** azines are 3-4 D in the gas phase (*12*) and the degree of alignment achieved in their crystals exceeds 90 percent of the optimal value (*20*). In all of the other unsymmetrical azine crystals that we have studied the monomers align such that complete dipole cancellation is observed and an example of this is **NH_2-NO_2** (Figures 3 and 4). The anti-parallel dipole aligned crystals will never show any nonlinear optical properties, however they are important when discussing the directing effects of aromatic rings in the crystal structures of acetophenone azines. We only observe parallel and anti-parallel dipole alignment within the double T-contacts of our crystals. Never do we witness any intermediate crystal packing moieties. This high degree of anisotropy is achieved because the arene-arene double T-contact acts as an extremely efficient lateral synthon.

References

1. Zyss, J. *Molecular Nonlinear Optics, Materials, Physics, and Devices*; Academic Press, Inc.: New York, NY, 1994.
2. Sakamoto, M. *Chem. Eur. J.* **1997**, *3*, 684-689.
3. Walba, D. M.; Korblova, E.; Shao, R.; Maclennan, J. E.; Link, D. A.; Glaser, M. A.; Clark, N. A. *Science* **2000**, *288*, 2181-2184.
4. Trzaska, S. T.; Hsu, H. F.; Swager, T. M. *J. Am. Chem. Soc.* **1999**, *121*, 4518-4519.
5. Simoni, F.; Francescangeli, O. *J. Phys. Condens. Matter* **1999**, *11*, R439-R487.
6. Atassi, Y.; Chauvin, J.; Delaire, J. A.; Delouis, J.-F.; Fanton–Maltey, I.; Nakatani, K. *Pure & Appl. Chem.* **1998**, *70*, 2157-2166.
7. Kurabayashi, K.; Goodson, K. E. *J. Appl. Phys.* **1999**, *86*, 1925-1931.
8. Saad, B.; Galstyan, T. V.; Dinescu, L.; Lemieux, R. P. *Chem. Phys.* **1999**, *245*, 395-405.
9. Luty, T.; Eckhardt, C. J. *J. Phys. Chem.* **1996**, *100*, 6793-6800.
10. Kohler, B. E.; Wohl, J. C. *J. Chem. Phys.* **1995**, *102*, 7773-7781.
11. Geissinger, P.; Kohler, B. E.; Woehl, J. C. *J. Phys. Chem.* **1995**, *99*, 16527-16529.
12. Glaser, R.; Chen. G. S. *J. Comput. Chem.* **1998**, *19*, 1130-1140.
13. Lewis, M., PhD Dissertaion, University of Missouri, **2001**.
14. Chen, G. S.; Wilbur, J. K.; Barnes, C. L.; Glaser, R. *J. Chem. Soc. Perkin Trans. 2* **1995**, 2311-2317.
15. Glaser, R.; Chen, G. S.; Anthamatten, M.; Barnes, C. L. *J. Chem. Soc. Perkin Trans. 2* **1995**, 1449-1458.
16. Glaser, R.; Chen, G. S.; Barnes, C. L. *J. Org. Chem.* **1993**, *58*, 7446-7455.
17. Lewis, M.; Barnes, C. L.; Hathaway, B. A.; Glaser, R. *Acta Cryst. C* **1999**, *55*, 975-978.
18. Lewis, M.; Barnes, C. L.; Glaser, R. *J. Chem. Crystallogr.* **1999**, *29*, 1043-1048.
19. Lewis, M.; Barnes, C. L.; Glaser, R. *Acta Cryst. C* **2000**, *56*, 393-396.
20. Lewis, M.; Barnes, C. L.; Glaser, R. *J. Chem. Crystallogr.* **2001**, *31*, in press.
21. Lewis, M.; Barnes, C. L.; Glaser, R. *Can. J. Chem.* 1998, **76**, 1371-1378.
22. Battaglia, M. R.; Buckingham, A. D.; Williams, J. H. *Chem. Phys. Lett.* **1981**, *78*, 421-423.
23. Waschull, J.; Heiner, Y.; Sumpf, B.; Kronfeldt, H. D. *J. Mol. Spectrosc.* **1998**, *190*, 140-149.
24. Cox, E. G. *Proc. Roy. Soc.* **1932**, *A135*, 491.
25. Kochikov, I. V.; Tarasov, Y. I.; Kuramshina, G. M.; Spiridonov, V. P.; Yagola, A. G.; Strand, T. G. *J. Mol. Struc.* **1998**, *445*, 243-258.
26. Wu, Z.; Glaser, R., to be published.
27. Hobza, P.; Selzle, H. L.; Schlag, E. W. *Chem. Rev.* **1994**, *94*, 1767-1785.
28. Garrett, A. W.; Zwier, T. S. *J. Chem. Phys.* **1992**, *96*, 3402-3410.
29. Hobza, P.; Selzle, H. L.; Schlag, E. W. *J. Chem. Phys.* **1990**, *93*, 5893-5897.
30. Hobza, P.; Selzle, H. L.; Schlag, E. W. *J. Phys. Chem.* **1993**, *97*, 3937-3938.
31. Hobza, P.; Selzle, H. L.; Schlag, E. W. *J. Am. Chem. Soc.* **1994**, *116*, 3500-3506.
32. Hobza, P.; Selzle, H. L.; Schlag, E. W. *J. Phys. Chem.* **1996**, *100*, 18790-18794.

33. Spirko, V.; Engkvist, O.; Soldan, P.; Selzle, H. L.; Schlag, E. W.; Hobza, P. *J. Chem. Phys.* **1999**, *111*, 572-582.
34. Chipot, C.; Jaffe, R.; Maigret, B.; Pearlman, D. A.; Kollman, P. A. *J. Am. Chem. Soc.* **1996**, *118*, 11217-11224.
35. Jorgensen, W. L.; Severance, D. L. *J. Am. Chem. Soc.* **1990**, *112*, 4768-4774.
36. Allinger, N. L.; Lii, J.-H. *J. Comp. Chem.* **1987**, *8*, 1146-1153.
37. Steed, J. M.; Dixon, T. A.; Klemperer, W. *J. Chem. Phys.* **1979**, *70*, 4940-4946.
38. Janda, K. C.; Hemminger, J. C.; Winn, J. S.; Novick, S. E.; Harris, S. J.; Klemperer, W. *J. Chem. Phys.* **1975**, *63*, 1419-1421.
39. Hopkins, J. B.; Powers, D. E.; Smalley, R. E. *J. Phys. Chem.* **1981**, *85*, 3739-3742.
40. Law, K. S.; Schauer, M.; Bernstein, E. R. *J. Chem. Phys.* **1984**, *81*, 4871-4882.
41. Bornsen, K. O.; Selzle, H. L.; Schlag, E. W. *J. Chem. Phys.* **1986**, *85*, 1726-1732.
42. Ernstberger, B.; Krause, H.; Kiermeier, A.; Neusser, H. J. *J. Chem. Phys.* **1990**, *92*, 5285-5296.
43. Venturo, V. A.; Felker, P. M. *J. Chem. Phys.* **1993**, *99*, 748-751.
44. Henson, B. F.; Hartland, G. V.; Venturo, V. A.; Felker, P. M. *J. Chem. Phys.* **1992**, *97*, 2189-2208.
45. Scherzer, W.; Kratzschmar, O.; Selzle, H. L.; Schlag, E. W. *Z. Naturforsch. A* **1992**, *47*, 1248-1252.
46. Ebata, T.; Hamakado, M.; Moriyama, S.; Morioka, Y.; Ito, M. *Chem. Phys. Lett.* **1992**, *199*, 33-41.
47. Arunan, E.; Gutowsky, H. S. *J. Chem. Phys.* **1993**, *98*, 4294-4296.
48. Laatikainen, R.; Ratilainen, J.; Sebastian, R.; Santa, H. *J. Am. Chem. Soc.* **1995**, *117*, 11006-11010.
49. Cox, E. G.; Cruickshank, D. W. J.; Smith, J. A. S. *Proc. Roy. Soc. London Ser. A* **1958**, *247*, 1-21.
50. Bacon, G. E.; Curry, N. A.; Wilson, S. A. *Proc. Roy. Soc. London Ser. A* **1964**, *279*, 98-110.
51. Piermarini, G. J.; Mighell, A. D.; Weir, C. E.; Block, S. *Science* **1969**, *165*, 1250-1255.
52. Eliel, E. L.; Wilen, S. H.; Mander. L. N. *Stereochemistry of Organic Compounds*; John Wiley & Sons Inc.: New York, 1994, p. 1120.